A BANDLIMITED STEP FUNCTION FOR USE IN DISCRETE PERIODIC EXTENSION

by

SUREKA PATHMANATHAN

B.Sc., University of Peradeniya, 2010

A THESIS

submitted in partial fulfillment of the
requirements for the degree

MASTER OF SCIENCE

Department of Mathematics
College of Arts and Sciences

KANSAS STATE UNIVERSITY
Manhattan, Kansas

2013

Approved by:

Major Professor
Nathan Albin

Copyright

Abstract

A new methodology is introduced for use in discrete periodic extension of non-periodic functions. The methodology is based on a band-limited step function, and utilizes the computational efficiency of FC-Gram (Fourier Continuation based on orthonormal Gram polynomial basis on the extension stage) extension database. The discrete periodic extension is a technique for augmenting a set of uniformly-spaced samples of a smooth function with auxiliary values in an extension region. If a suitable extension is constructed, the interpolating trigonometric polynomial found via an FFT(Fast Fourier Transform) will accurately approximate the original function in its original interval. The discrete periodic extension is a key construction in the FC-Gram algorithm which is successfully implemented in several recent efficient and high-order PDEs solvers. This thesis focuses on a new flexible discrete periodic extension procedure that performs at least as well as the FC-Gram method, but with somewhat simpler implementation and significantly decreased setup time.

Table of Contents

Table of Contents iv

List of Figures vi

List of Tables ix

Acknowledgements ix

1 Introduction and Background 1

1.1 Introduction 1

1.2 Overview of Chapters 1

1.3 Background 2

1.3.1 Fourier Methods 2

1.3.2 Gibbs Ringing Phenomenon 3

1.3.3 Finite Difference Methods (FDM) 4

2 Background : Periodic Extension 5

2.1 Periodic extension in the continuum 5

2.1.1 Smooth extension 6

2.1.2 Windowing with compact support 7

2.1.3 Periodization 7

2.2 Discrete Periodic Extension 7

2.2.1 Fourier Extension Methods 8

2.3 Aim 11

3 Smooth Extension 12

4 Windowing 16

4.1 Smoothed top-hat window 18

4.2 Bandlimited Step 19

4.2.1 The Optimization Problem 21

5 Periodization 24

6 Numerical Experiments and Results 26

7 Conclusion 37

Bibliography 38

A Optimization problem of the bandlimited step function 42

B Coefficients of the bandlimited step function 47

List of Figures

1.1 Demonstration of Gibbs phenomenon of $f(x) = 1$ on $[-1, 1]$ and $f(x) = 0$ elsewhere on $[-\pi, \pi]$ for W=35 Fourier modes 3

2.1 In (a), a function on $[0, 1]$ is extended smoothly $\forall\ x \in \mathbb{R}$. The resulting function is multiplied by the windowing function (b) to produce a smooth extension (c) with a compact support on $[-\delta, 1 + \delta]$. In (d), this function is periodized to period c 6

2.2 Discretization of the domain $[0, 1]$ with N equispaced points 8

3.1 An illustration of the steps of smooth extension. $\mathbf{f}$ (light curve)denotes samples of original functions with N-N_l-N_r points. $\mathbf{f_l}$ and $\mathbf{f_r}$ (thick black curves) represent samples used for polynomial approximation p_l and p_r with N_l and N_r samples respectively. f_{e_l} andf_{e_r} represent M values of smooth extension (open circles) using f_l and f_r respectively 13

4.1 In(a), extended polynomial function with degree = 1 using FC-Gram method and associated 'implicit' windowing function in (b) 17

4.2 In (a) , a smooth step function transitioning between the values 0 and 1 at α and $1-\beta$ respectively. In (b), the sampling of the step at $M = 25$ equispaced nodes in the interval $(\alpha, 1 - \beta)$ 20

4.3 Discrete Fourier coefficient magnitudes of a smooth function $f_1'(x)$ and a (mildly) discontinuous function $f_2'(x)$ 21

5.1 Overlapping extension example for the Periodization defined on Equation 5.1 24

6.1 In(a), the extended function using FC-Gram method for a polynomial with degree=2. The original function and associated 'implicit' window function are respectively in (b) & (c). Similarly, (d) (e) and (f) are for degree 3. . . . 27

6.2 In(a), the extended function using FC-Gram method for a polynomial with degree=4. The original function and associated 'implicit' window function are respectively in (b) & (c). Similarly, (d) (e) and (f) are for degree 5. . . . 28

6.3 In(a), the extended function using FC-Gram method for a polynomial with degree=6. The original function and associated 'implicit' window function are respectively in (b) & (c). Similarly, (d) (e) and (f) are for degree 7. . . . 29

6.4 In(a), the extended function using FC-Gram method for a polynomial with degree=8. The original function and associated 'implicit' window function are respectively in (b) & (c). Similarly, (d) (e) and (f) are for degree 9. . . . 30

6.5 Comparison of window functions . In (a), the points labeled 'FC-Gram' indicate the implicit step function obtained when applying the original FC-Gram with $M = 25$ points. The points labeled 'band-limited' indicate the smooth step-up function ψ described in Section 4.2.1 with $M = 25$ extension points and $\alpha = \beta = 10/68, W = 33$. In (b), similar comparison is reproduced with additional band-limited step for $\alpha = \beta = 0.15, W = 29$ 32

6.6 In (a), the representation error observed when applying discrete periodic extensions to the function $f_1(x)$ (b). The points labeled 'FC-Gram' indicate the results of applying the original FC-Gram algorithm with $M = 25$ points. The points labeled 'band-limited' indicate the results of applying the new periodic extension developed in this work using bandlimited step function developed in Section 4.2.1 with $M = 25$ extension points 33

6.7 In (a), the representation error observed when applying discrete periodic extensions to the function $f_2(x)$ (b). The points labeled 'FC-Gram' indicate the results of applying the original FC-Gram algorithm with $M = 25$ points. The points labeled 'band-limited' indicate the results of applying the new periodic extension developed in this work using bandlimited step function developed in Section 4.2.1 with $M = 25$ extension points 33

6.8 In (a), the representation error observed when applying discrete periodic extensions to the function $f_3(x)$ (b). The points labeled 'FC-Gram' indicate the results of applying the original FC-Gram algorithm with $M = 25$ points. The points labeled 'band-limited' indicate the results of applying the new periodic extension developed in this work using bandlimited step function developed in Section 4.2.1 with $M = 25$ extension points 34

6.9 Comparison of smooth extension of a function defined on [0,1], using FC-Gram method and new periodic extension developed in this work 35

6.10 In (a), non-overlapping discrete periodic extension of function $f_4(x)$ for the periodization as in Equation (3.4) and in (b) overlapping extension for a small period as defined in Equation (5.1) 35

A.1 The windowing function ϕ as defined on Equation (4.1) 42

A.2 The bandlimited step-up function ψ on [0,1] (dotted line shows the transition region) 43

List of Tables

6.1 The set of 'best-fit' window paramenters of the band-limited step function ψ 31

Acknowledgments

I am extremely grateful to my advisor, Dr. Nathan Albin , for his guidance and encouragement in all aspects of my work and career, and of course, for his patience. I would like to thank my committee members, Dr. Bala Natarajan and Dr. Hrant Hakobyan. I am also grateful to my parents. Without them, I would not have climbed the ladder this much. I would like to thank my fiancé and my close friends for their support throughout these years.

Chapter 1

Introduction and Background

1.1 Introduction

This thesis presents a simplified discrete periodic extension scheme that performs at least as well as FC-Gram (Fourier continuation based on Gram polynomials) method. The discrete periodic extension is a technique used to extend the samples of a given smooth function with auxiliary values in an extension region. In recent years there have been several methods introduced in [3, 4, 8, 10, 23, 25] to solve partial differential equations (PDEs) and there are considerable improvements on developing variety of efficient high-order- accurate PDE solvers utilizing FC-Gram algorithms (Ref [3, 10, 23]). According to the author's knowledge, there is no known "best" recipe to achieve 'stable' solvers for arbitrary domains. This research is focused on finding a replacement for more - complex FC-Gram algorithm to allow more freedom on PDE solver development.

1.2 Overview of Chapters

A brief overview of a few existing methods utilized in PDE solvers and Gibbs ringing phenomenon is presented in the remainder of this Chapter. Chapter 2 presents a brief overview

of periodic extension techniques on the continuum version as well as the discrete version. The main work, organized by a three-step procedure to construct the discrete extension is presented in Chapters 3 to 5. The numerical results are presented in Chapter 6 and the thesis is concluded in Chapter 7.

1.3 Background

1.3.1 Fourier Methods

If a function $f(x)$ is periodic on $[0,1]$ sampled at n evenly spaced points $\{x_j\}$ where $x_j = j/n \quad j = 0, 1, \ldots, n-1$, then $f(x)$ can be approximated by a finite Fourier sum of the form

$$f(x_j) = \frac{1}{N} \sum_{k=-\lfloor N/2 \rfloor}^{\lceil N/2 \rceil - 1} a_k \exp(2\pi i k x_j) \tag{1.1}$$

where

$$a_k = \sum_{j=0}^{n-1} f(x_j) e^{-2\pi i x_j k} \tag{1.2}$$

The computations in Equations (1.1) & (1.2) are accelerated by FFT. Of course, the convergence of such Fourier Series approximation depends on the smoothness of the function in its domain.(see [11, 14, 16, 22])

If $f(x)$ is not periodic, then the finite Fourier sums converge pointwise to f on the open interval $(0,1)$ and the finite Fourier sum experience ripples at the boundaries - Gibbs phenomenon.

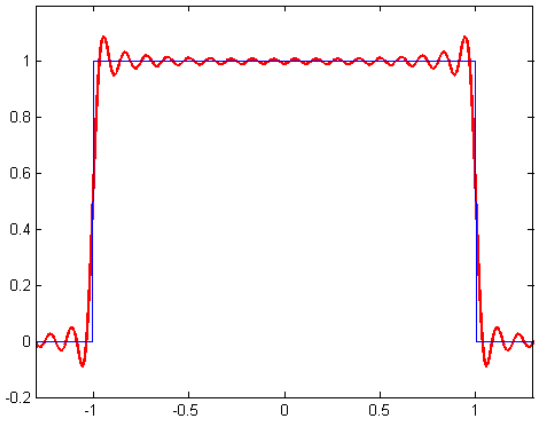

Figure 1.1: Demonstration of Gibbs phenomenon of $f(x) = 1$ on $[-1, 1]$ and $f(x) = 0$ elsewhere on $[-\pi, \pi]$ for W=35 Fourier modes

1.3.2 Gibbs Ringing Phenomenon

Consider the periodic function $f(x)$ defined on previous section and if $f(x)$ is not periodic, the finite Fourier sum exhibits the Gibbs phenomenon in the vicinity of discontinuities. As n increases the ripples in the partial sums become compressed toward the discontinuity, but the peak amplitude of these ripples does not decrease with increasing n. Figure 1.1 shows an example of the Gibbs ringing effect for $f(x) = 1$ on $[-1, 1]$ and $f(x) = 0$ elsewhere on $[-\pi, \pi]$.

In past decades, approaches have been made to resolve Gibbs phenomenon. Earlier contributions include low-pass filtering of high-order Fourier coefficients [24] : one of the noted developments was based on Gegenbauer polynomial methods (see [15] for more details). Some of the methods involves reprojecting the oscillating Fourier functions into an alternate orthogonal basis in order to minimize overshoot attain convergence [13]. However these algorithms require prior knowledge of the singularities of the function and its derivatives. The Fourier extension method proposed in [5] towards the resolution of this effect, basically involves the construction of a periodic extension of the original function on a larger interval. An overview of the methods based on Fourier extension technique will be discussed in the

following Chapter.

1.3.3 Finite Difference Methods (FDM)

Finite difference methods are one of the most well-known methods used to find numerical solutions to initial boundary-value PDEs. FDMs are obtained by replacing the spatial derivatives in a differential equation with finite difference approximations. The 'order of accuracy' of FDMs is estimated by means of Taylor series approximation (Ref [18, 19, 30]). FDMs are easy to develop with the use of biased/non-biased stencils. Although, the implementation of high-order FD solvers is straightforward, achieving stability and accuracy at the boundaries may not be possible in all general domains. (see [3, 20, 25, 26, 27, 29, 31] for detailed discussion.)

Chapter 2

Background : Periodic Extension

2.1 Periodic extension in the continuum

Let $f(x)$ be a smooth non-periodic function on $[0,1]$ ($f \in C^k$, for example with $k = 10$ or $k = 20$), and assume a smooth periodic extension $\widetilde{f}(x)$ can be found on larger interval $[-x_l, 1 + x_r]$ with the property that $\widetilde{f}(x)$ is a good approximation of $f(x)$ (for example, $\widetilde{f}(x) - f(x)$ is small in a suitable Sobolev norm), which we denote by $\widetilde{f}(x) \approx f(x)$ for all x in $[0,1]$. Note, the function $f(x)$ can be translated to a domain $[a,b] \quad \forall a, b \in \mathbb{R}$ with suitable scaling and shifting.

In this context such a periodic extension is referred to as a *periodic extension in the continuum* in order to distinguish it from the discrete analog discussed later in this work. The periodic extension in the continuum has been treated in [1, 2, 5, 16] and related results are presented in [6, 17].

The three-step procedure used in the continuum method is,

- Smooth extension
- Windowing with compact support

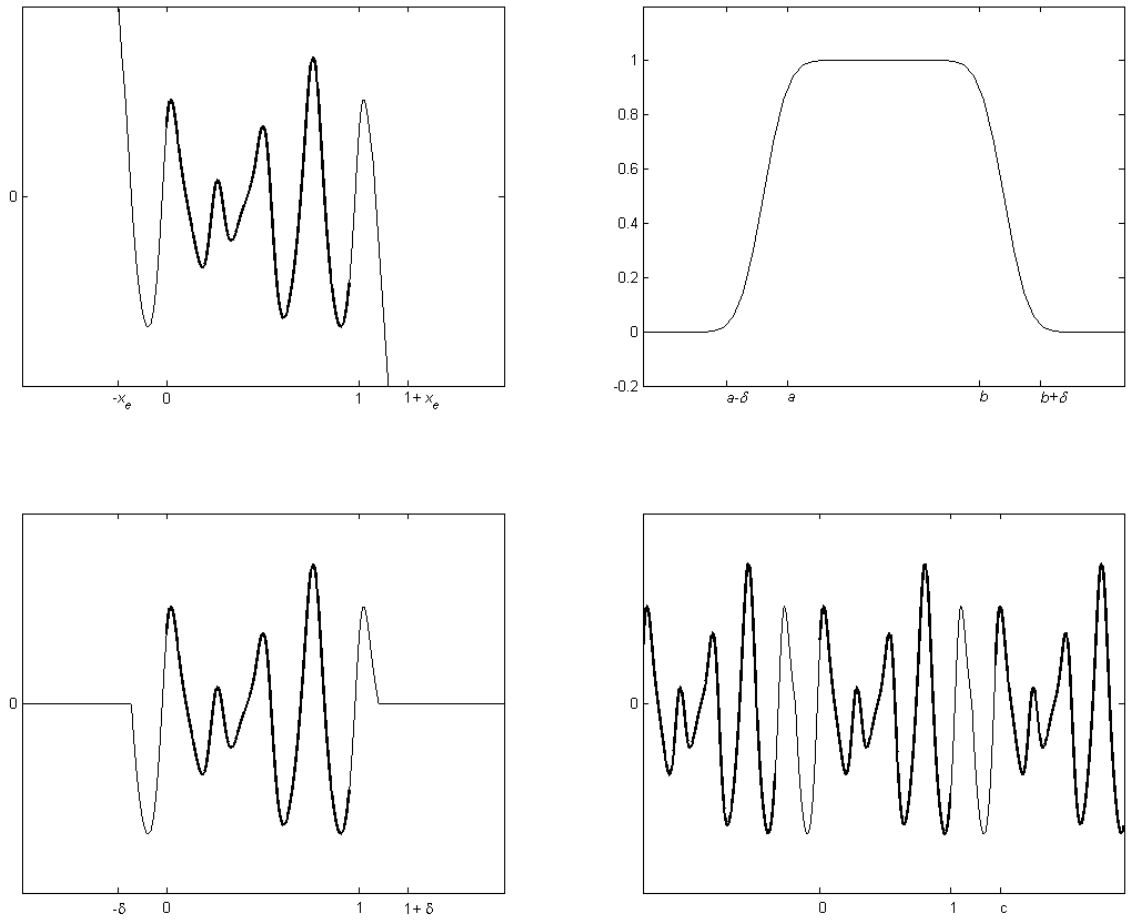

Figure 2.1: In (a), a function on $[0, 1]$ is extended smoothly $\forall\, x \in \mathbb{R}$. The resulting function is multiplied by the windowing function (b) to produce a smooth extension (c) with a compact support on $[-\delta, 1 + \delta]$. In (d), this function is periodized to period c .

- Periodization

2.1.1 Smooth extension

Let f be a function on $[0, 1]$. As defined above assume f and several of its derivatives are continuous and bounded on $[0, 1]$. A smooth extension of $f(x)\ \forall\ x \in \mathbb{R}$ can be found by applying the Taylor series approximation; i.e. given a smooth function f on $[0, 1]$ there exist

a smooth extension function f_{ext} on all of $\mathbb{R}$ with the property,

$$f_{\text{ext}}(x) = f(x) \qquad \text{for } \forall x \in [0,1]$$

2.1.2 Windowing with compact support

Once the function $f(x)$ is smoothly extended to $f_{\text{ext}}(x)$, a compact support $[-\delta, 1+\delta]$ can be easily applied to $f_{\text{ext}}(x)$ to form a windowed extension function (see Figure 2.1(c)). The windowed extension $f_{w_{\text{ext}}}$ can be formulated as

$$f_{w_{\text{ext}}}(x) = \phi(x)\, f_{\text{ext}}(x) \qquad \text{supp}(f_{w_{\text{ext}}}(x)) \subseteq [-\delta, 1+\delta]$$

with $f_{w_{\text{ext}}}(x) = f(x) \quad \text{for } x \in [0,1]$

2.1.3 Periodization

Lastly, the windowed smooth extension $f_{w_{\text{ext}}}(x)$ can be periodized into a smooth periodic extension $f_{\text{per}}(x)$ with period $c > 0$:

$$f_{\text{per}}(x) = \sum_{k=-\infty}^{\infty} f_{w_{\text{ext}}}(x + kc) \qquad c \geq (1+\delta)$$

with the property that

$$f_{\text{per}}(x) = f(x) \text{ for } x \in [0,1].$$

2.2 Discrete Periodic Extension

The three-step procedure of continuum extension described in the previous section, motivates a new discrete construction. The periodic extension on the continuum extends the non-periodic function to a smooth periodic function on a larger domain, while the discrete

version deals with extending a *vector* of discrete samples of a non-periodic function to a vector of discrete samples of smooth periodic function on a larger interval. In fact, this extended vector can be viewed as samples of the periodized extended function $f_{\text{per}}(x)$ in Section 2.1.3.

In other words, the problem can be restated as follows:

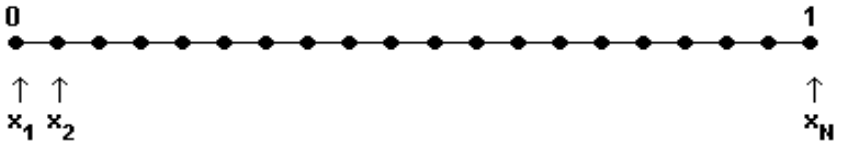

Figure 2.2: Discretization of the domain $[0, 1]$ with N equispaced points

Let $f(x)$ be smooth function on $[0, 1]$ that has been sampled at N equidistant points with the step size $\eta = \dfrac{x_N - x_1}{N-1}$, $x_1 = 0$ and $x_N = 1$. Let the vector of samples on $[0, 1]$ be denoted as $\mathbf{f} \in \mathbb{R}^N$ where $\mathbf{f} = (f_j)$, $f_j = f(x_j)$ with $x_j = x_1 + (j-1)\eta$ $(j = 1, 2, \ldots, N)$. Then an extended vector $\widetilde{\mathbf{f}} = (\widetilde{f}_j) \in \mathbb{R}^{N+N_e}$ with the property $\widetilde{f}_j = f_j$ for $j = 1, 2, \ldots, N$ needs to be found (here N_e is the number of samples at the extension region).

Although, any choice of $\{f_j\}_{N+1}^{N+N_e}$ will produce discrete periodic extension $\widetilde{\mathbf{f}}$, it is necessary to assure $\tilde{f}(x) \approx f(x) \quad \forall x \in [0, 1]$. Also, it is necessary to expect the discrete Fourier coefficients of $\widetilde{f}$ decay rapidly to zero, to attain good approximation with few samples (N_e) at the extension region.

2.2.1 Fourier Extension Methods

As discussed above, given a set of samples of a smooth function $f(x)$ on $[0, 1]$, we seek samples of an extended function on a larger interval $[-x_e, 1 + x_e]$. In other words, the goal is to produce Fourier coefficients $\{\widehat{f}_k\}_{k=-W}^{W}$ of a band-limited, $T\,(> 1)$ periodic function $\widetilde{f}$

such that,

$$\tilde{f}(x) = \sum_{k=-W}^{W} \widehat{f}_k \exp(i2\pi kx/T) \qquad T = 1 + 2x_e \tag{2.1}$$

where $\widetilde{f}(x) \approx f(x)$ on $[0, 1]$.

Although,the bandwidth W is unspecified, it is important to keep W as small as possible to maintain efficiency in FFT-based algorithms. In the past, there have been significant advances on Fourier extension methods (Ref [3, 4, 5, 6, 7, 8, 9, 10, 21]). We will be reviewing few Fourier extension methods related to our work, in the following sections.

(a) Fourier extension using a smooth window.

Let $f(x)$ be a nonperiodic function on $[0, 1]$, Fourier extension $\tilde{f}(x)$ using C^∞- bell window is :

$$\tilde{f}(x) = \begin{cases} f(x) & x \in [0, 1] \\ f(x)\, w(x) & x \in [-x_{\text{ext}}, 0) \cup (1, 1 + x_{\text{ext}}] \end{cases}$$

where $w(x)$ is equal to 1 in the original domain $[0, 1]$, analytic everywhere on the extended interval $[x_{\text{ext}}, 1 + x_{\text{ext}}]$ and is 'infinitely flat' (i. e. w and all of its derivatives zero) at $x = 0, 1, -x_{\text{ext}}, 1 + x_{\text{ext}}$.Overview of this 'smoothed top-hat window' is delayed until Chapter 4.

It is important to note that, $\tilde{f}(x)$ claimed to produce exponentially convergent and accurate approximations [5, 6]. But this extension requires that f needs to be known in the extended region and real analytic. In many applications, however, $f(x)$ is known only in the original domain $[0, 1]$.

(b) FC-SVD Method

As in the original context [7], let us define $f(x)$ be nonperiodic smooth function on $[0, 1]$ and $f \in C^k([0, 1])$ with either k positive or $k = \infty$. Also let x_j be discrete points on $[0, 1]$ for $j = 1, 2, \ldots, N$ with $x_1 = 0, x_N = 1$. Further consider a larger interval $[0, b]$ where $b > 1$, then a b-periodic continued function $\tilde{f}(x)$ is produced by a certain least-squares

approximations of f by trigonometric polynomials where,

$$\tilde{f}(x) = \sum_{k=-\lceil W/2 \rceil+1}^{\lceil W/2 \rceil} a_k \exp(2\pi i k x/b)$$

Finding the optimal solution to the least square problem

$$\min \sum_{j=1}^{N} \left(\sum_{k=-\lceil W/2 \rceil+1}^{\lceil W/2 \rceil} a_k \exp(2\pi i k x_j/b) - f(x_j) \right)^2$$

by solving for coefficient a_k using a regularized Singular-Value Decomposition(SVD) yields an approximation [7, 9]. Due to the conditioning of this linear system, FC-SVD continuation method loses very little accuracy compared to other Gibbs resolution techniques [20]. However, implementing the FC-SVD method in PDEs solvers is computationally expensive (see Ref [10, 20, 22]).

(c) FC-Gram Method

One of the recent developments which succeeded in producing PDEs solvers is the FC-Gram approach which basically maintains a balance between high-order accuracy and stability in solvers for boundary-value PDEs. The FC-Gram algorithm was introduced in [10] where 'Gram' represents the use of orthonormal Gram polynomial basis in the extension stage. Advantages over FC-SVD method is discussed in detail in Ref [10, 20, 22].

Let us consider once again $f \in C^k$ nonperiodic function on $[0, 1]$ sampled at N equidistant points. This algorithm is based on smooth boundary functions f_{left} and f_{right} where f_{left} is defined on $C^k\,[1-\delta, 1]$ and f_{right} is defined on $C^k\,[0, \delta]$ and shifted to $[b, b+\delta]$. Depending on $f_{\text{left}}(x_i)$ and $f_{\text{right}}(x_i)$, smooth extension $f_{\text{ext}}(x_i)$ needs to be evaluated for n_{ext} grid points on $[1, b]$, where $f_{\text{left}}(x_i)$ are samples of right-most n_δ grid values and $f_{\text{right}}(x_i)$ are samples of left-most n_δ grid values. These boundary functions f_{left} and shifted f_{right} are projected

orthogonally onto elements of f^p_{left} and f^p_{right} of Gram polynomial subspaces. Finally, $f_{\text{ext}}(x)$ is obtained on the interval $[1-\delta, b+\delta]$ by taking linear combination of certain continuations formed by f^p_{left} and f^p_{right} .

The efficient implementation of this method depends on two phases : *offline*, the precomputation and *online*, construction of Fourier continuation in any arbitrary interval. In the offline phase, the matching extension function f_{ext} is precomputed by generating an extension database of the sets of $\{f^r\}_{r=0}^{n_\delta - 1}$ (where r is the degree of the polynomial and n_δ is the associated grid points) for the polynomial basis in the interval $[0, 1]$ in offline for future use in online phase.

2.3 Aim

Although FC-Gram method described in the previous section has been successfully implemented for a variety of high-order-accurate PDE-solvers, the complexity of the precomputation step is a reason to find a replacement. This precomputation requires approximations on auxiliary fine grids and the cost of computing the extension database is fairly considerable, as it requires very high precision evaluation using SVDs of large matrices (e.g. 32x91) . Despite the fact that the offline computation cost and the approximations do not impact the efficiency of the FC-Gram based solvers, it does complicate the freedom of solver development. This observation leads to an interesting question - is there any simplified discrete periodic extension algorithm which may act as a replacement for the more complex FC-Gram algorithm. The methodology presented here requires the solutions of much smaller (e.g. 18x18) linear systems, thus reducing the time required to compute the extension database from a few minutes to a few seconds. In addition, it allows much more freedom to perform parameter studies (e.g. number of grid points in the extension region, location of sample nodes) in the development of new FC-based PDE solvers.

Chapter 3

Smooth Extension

The first step of the discrete periodic extension is a discrete version of the smooth extension of Section 2.1.1 (a) : generating the samples of a smooth extended function $\widetilde{f}(x)$ with $\widetilde{f}_j = \widetilde{f}(x_j)$ where $\widetilde{f}(x_j) = f(x_j), \forall x_j \in [0,1]$. More precisely, given the vector $\mathbf{f} \in \mathbb{R}^N$, the extension vector $\widetilde{\mathbf{f}}$ is the extrapolated sequence $\{\widetilde{f}_j\}_{j=-\infty}^{\infty}$ with the property $\widetilde{f}_j = f_j$ for $j = 1, 2, \ldots, N$.

Since our main concern of this work is to find a simplest way to produce similar results as the FC-Gram approach, like in [10, 21] we will also restrict our extension using *'near-boundary'* values $\{f_1, f_2, \ldots, f_{\mathrm{N_l}}\}$ near $x = 0$ and $\{f_{\mathrm{N-N_{r+1}}}, f_{\mathrm{N-N_{r+2}}}, \ldots, f_{\mathrm{N}}\}$ near $x = 1$ where N_l and N_r are the number of discrete points near the left and right boundaries respectively. The extension is based on the values of the interpolating polynomials near these two boundary values.

Given N_l samples, there exist a unique polynomial $p_l(x_j)$ with degree of $p_l(x_j)$, $d_l \leq N_l - 1$, passing through those N_l values such that $p_l(x_j)$ act as an interpolation of $f(x_j)$ near $x = 0$ and as an extrapolation of $f(x_j)$ for $x_j \in (-\infty, 0)$. Similarly, $p_r(x_j)$ can be

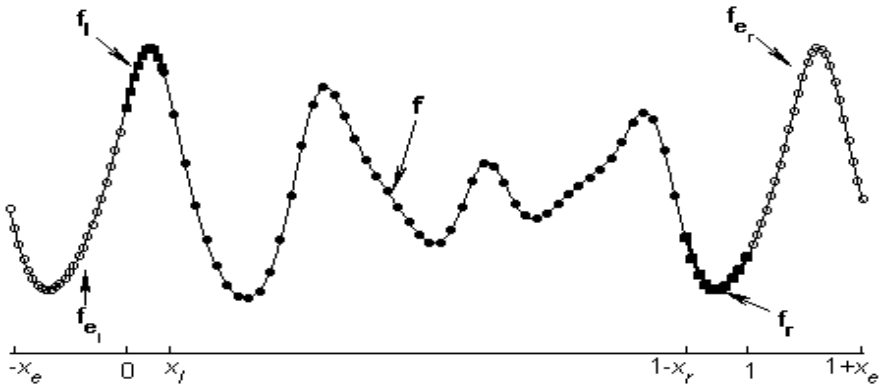

Figure 3.1: An illustration of the steps of smooth extension. $\mathbf{f}$ (light curve)denotes samples of original functions with N-N_l-N_r points. $\mathbf{f_l}$ and $\mathbf{f_r}$ (thick black curves) represent samples used for polynomial approximation p_l and p_r with N_l and N_r samples respectively. f_{e_l} andf_{e_r} represent M values of smooth extension (open circles) using f_l and f_r respectively

defined near $x = 1$. Then define the extension as,

$$\widetilde{f}(x_j) = \begin{cases} p_l(x_j) & \text{if } x_j \in (-\infty, 0) \\ f(x_j) & \text{if } x_j \in [0, 1] \\ p_r(x_j) & \text{if } x_j \in (1, \infty) \end{cases}$$

As explained in Section 2.1, the extended sequence $f_{\text{ext}}(x_j) = \widetilde{f}(x_j)$ will eventually be multiplied by a window function $\phi(x)$ with compact support. Hence, only a finite number of $\{\widetilde{f}_j\}$ values ever need to be computed. Henceforth, we assume $\mathbf{f} \in \mathbb{R}^N$ is extended to a new vector $\widetilde{\mathbf{f}} \in \mathbb{R}^{N+2M}$ where M is the number of grid points in the window's transition region ($[-x_e, 0], [1, 1 + x_e]$).

This operation can be re-expressed into a convenient form by using Gram polynomial bases. We form the Gram polynomial basis $\{q^l_{j-1}\}_{j=1}^{d_{l+1}}$ by applying Gram-Schmidt orthonor-

malization process to the monominal basis $\{1, x, \ldots, x^{d_l}\}$ with inner product

$$\langle p, q \rangle = \sum_{j=1}^{N_l} p(x_j) q(x_j).$$

The polynomial near the left boundary can be written as,

$$p_l(x) = \sum_{j=1}^{d_{l+1}} \langle p_l, q_{j-1}^l \rangle \, q_{j-1}^l(x)$$

So, the extension polynomial Ep_l is as follows,

$$Ep_l(x) = \sum_{j=1}^{d_l+1} \langle p_l, q_{j-1}^l \rangle \, q_{j-1}^l(x) \tag{3.1}$$

Similarly, $p_r(x)$ and $Ep_r(x)$ can be defined. Therefore, the smooth extrapolation of near-boundary functions f_l and f_r are as follows: (see Figure 3.1)

$$f_{e_l} = E_l Q_l^T f_l$$

$$f_{e_r} = E_r Q_r^T f_r$$

where Q_l is an orthogonal $N_l \times N_l$ matrix with the values

$$(Q_l)_{ij} = q_{j-1}^l(x_i) \qquad i, j = 1, 2, \ldots, N_l \tag{3.2}$$

and E_l is an $M \times N_l$ matrix with the entries

$$(E_l)_{ij} = q_{j-1}^l \left(x_{i-M}\right) \qquad i = 1, 2, \ldots, M \qquad j = 1, 2, \ldots, N_l \tag{3.3}$$

Matrices Q_r and E_r are defined analogously.
Writing $\mathbf{f} = \{f_l, f_c, f_r\}^T$ where $f_l \in \mathbb{R}^{N_l}$, $f_r \in \mathbb{R}^{N_r}$ and $f_c \in \mathbb{R}^{N-N_l-N_r}$, then the extension

vector $\widetilde{\mathbf{f}} = \{f_{e_l}, f_l, f_c, f_r, f_{e_r}\}^T$ can be represented in a matrix form.

$$\begin{pmatrix} f_{e_l} \\ f_l \\ f_c \\ f_r \\ f_{e_r} \end{pmatrix} = \begin{pmatrix} E_l Q_l^T & 0 & 0 \\ I & 0 & 0 \\ 0 & I & 0 \\ 0 & 0 & I \\ 0 & 0 & E_r Q_r^T \end{pmatrix} \times \begin{pmatrix} f_l \\ f_c \\ f_r \end{pmatrix} \tag{3.4}$$

Notice that as discussed in [3, 4], *biased-extension* can be produced using different left-most and right-most grid points, N_l and N_r. For simplicity, we can choose N_l and N_r to be equal, say N_d

Although the Gram - Schmidt orthonormalization of polynomials and the extension of those polynomials involve poorly-conditioned computations, these computations take place during the offline phase and thus evaluations of Q_l, E_l, Q_r and E_r should be performed in very-high-precision, as is done in the original FC-Gram construction.

Chapter 4

Windowing

Since our focus is to find a simplified algorithm that performs as the original FC-Gram construction, it is interesting to observe the relatioship between the extended function and the original function. As explained in original context of FC-Gram method, a windowing function is not a part of the FC-Gram method (see Ref [20] for more details). However, the FC-Gram continuation exhibits a behavior of an 'implicit' windowing function in its extension. Figure 4.1 shows an example of such implied windowing function of FC-Gram for a polynomial function with degree = 1 . In Chapter 6, we present this relationship results for the polynomial functions of degrees 2 to 9.

Although, the FC-Gram method does not require windowing, its implicit window function exhibits a transition to zero either from 1 or -1 (see Figures 6.1 to 6.4), and it blends the continuation function to zero. This observation leads us to the discrete version of second step of smooth extension of Section 2.1 - i.e. the extended vector $\widetilde{\mathbf{f}}$ found in previous section can now be blended to zero on either end by multiplying with a suitable window function (see Figure 2.1 (b)). The shape of the windowing function is determined by its behavior in the transition region $[-\delta, 0] \cup [1, 1+\delta]$. Thus, the smooth window is determined by a smooth 'step-up' and a smooth 'step-down' by symmetry.

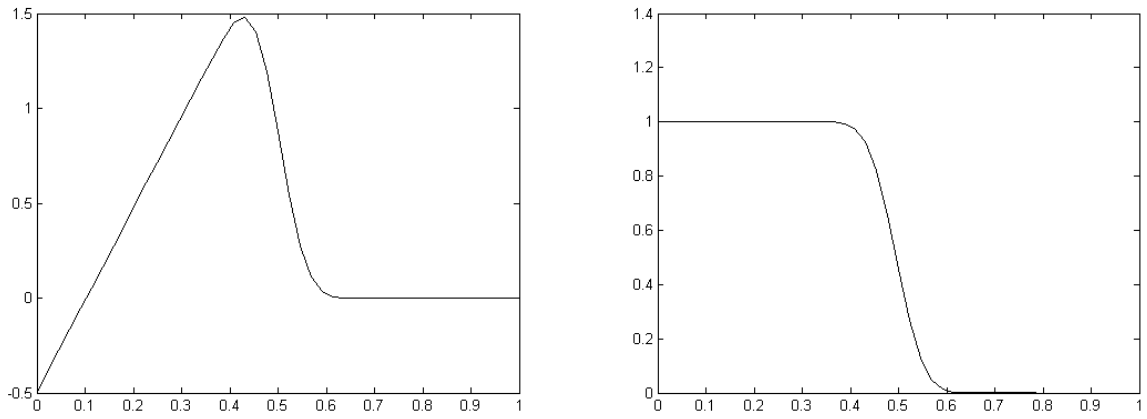

Figure 4.1: In(a), extended polynomial function with degree = 1 using FC-Gram method and associated 'implicit' windowing function in (b)

Let us define the window function $\phi(x, \delta)$ as,

$$\phi(x,\delta) = \begin{cases} 0 & x \in (-\infty, -\delta] \cup [1+\delta, \infty) \\ 1 & x \in [0,1] \\ \psi\left(\left(\dfrac{1-\beta-\alpha}{\delta}\right)x + (1-\beta)\right) & x \in [-\delta, 0) \\ \psi\left(-\left(\dfrac{1-\beta-\alpha}{\delta}\right)(x-1) + (1-\beta)\right) & x \in (1, 1+\delta] \end{cases} \tag{4.1}$$

where $\psi(x)$ shown in Figure 4.2, is a step-up function on $[\alpha, 1-\beta]$, $\psi(\alpha) = 0$, and $\psi(1-\beta) = 1$.

As mentioned in the previous chapter, it is sufficient to have M grid points in the transition region. Let us consider M samples of ψ in the transition region $(\alpha, 1-\beta)$ to be $\psi(\alpha + ih)$ with the step size $h = \dfrac{1-\beta-\alpha}{M+1}$ for $i = 1, \ldots, M$. These samples are then multiplied with E_l and E_r found in Chapter 3 to produce discrete windowed extension :

$$\widetilde{f}_w = E_w f = \begin{pmatrix} \overline{E}_l Q_l^T & 0 & 0 \\ I & 0 & 0 \\ 0 & I & 0 \\ 0 & 0 & I \\ 0 & 0 & \overline{E}_r Q_r^T \end{pmatrix} \times \begin{pmatrix} f_l \\ f_c \\ f_r \end{pmatrix} \tag{4.2}$$

where

$$\left(\overline{E}_l\right)_{ij} = \psi(\alpha + ih)\, q_{j-1}^l(x_{i-M}), \;\; i = 1, 2, \ldots, M, \;\; j = 1, 2, \ldots, d_l \tag{4.3}$$

($\overline{E}_r$ is computed in a similar manner).

In order to produce $\widetilde{f}_w$, we need to choose the step function $\psi(x)$, which determines the window function $\phi(x)$. But $\phi(x)$ needs to be picked in such a way that efficiency and stability are balanced. To maintain stability at the tails of $\widetilde{f}_w$, polynomial growth in the extended domain needs to be controlled, which leads $\phi(x)$ to have a rapid decay to zero. Moreover considering the efficiency on producing $\widetilde{f}_w$, the transition region of $\psi(x)$ needs to have as few points as possible to keep the FFT computation cheap. The FC-Gram extension [10] demonstrates that $M = 25$ points is sufficient enough in the transition region for high accuracy. By considering these requirements, $\psi(x)$ can be constructed with fixed M (for any large value of N)

This suggests, $\overline{E}$ and Q matrices can be precomputed once, for fixed M, in very high precision and stored as double data type to be reused for any value of N. Thus it is sufficient to consider the possible window functions ϕ , for fixed M. The following Section focuses on two such possibilities.

4.1 Smoothed top-hat window

Earlier in Section 2.2.1 (a) we described a Fourier periodic extension method which utilizes a smoothed top-hat (C^∞ - bell) window (see Ref [5, 6]). The aforementioned window $w(x)$

is based on the erf-like function: $w(x) = erf(Lx/\sqrt{1-x^2})$ (see Figure 1 of Ref [6])

In the Ref [6], the argument has been made on choosing an optimal L which, minimizes the error in truncating the Fourier series of the window function at the mode W. The optimal choice is determined to be

$$L = 0.911\sqrt{(1-r)W}$$

where r is the ratio of the length of domain of interest to the length of the extended interval. As it was in the previous discussion, for a fixed M, $1 - r \approx 2Mh$ where, $h = 1/(N-1) \approx 1/N$. By truncating at the Nyquist frequency we obtain, $W \approx (N + 2M)/2$. Thus, in the present setting, the optimal L is approximately

$$L \approx 0.911\sqrt{2Mh\,W} \approx 0.911\sqrt{W}$$

Figure 2 of Ref [6] indicates that L needs to be in the range of $4 - 6$ to resolve a smooth top-hat window which is identically equal to 1 on $[-1, 1]$ and is identically equal to 0 outside $[-\pi, \pi]$. The FC-Gram method in [10, 20] uses Nyquist frequency $W = 63$, which leads the choice of M which is approximately equal to $(63\,(1 - 1/\pi)) \approx 43$ points. But as we discussed in the previous section, the FC-Gram algorithm uses $M = 25$ points. Although the difference in computational cost of a C^∞-bell window with $M = 50$ extension points and FC-Gram method with $M = 25$ points is not very large, this observation leads us to seek another choice for the windowing function to achieve the same accuracy as FC-Gram with $M = 25$ points.

4.2 Bandlimited Step

The reason behind choosing an alternative window can be summarized by two principles and consequent remarks.

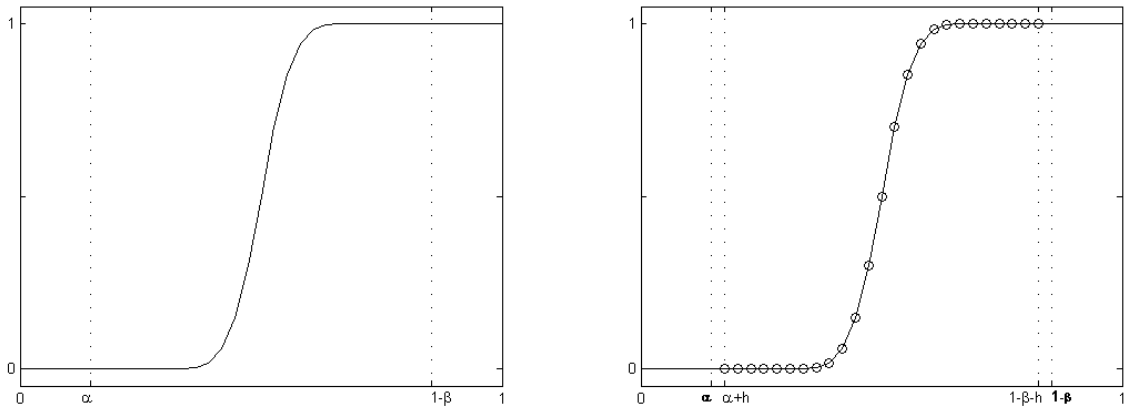

Figure 4.2: In (a) , a smooth step function transitioning between the values 0 and 1 at α and $1-\beta$ respectively. In (b), the sampling of the step at $M = 25$ equispaced nodes in the interval $(\alpha, 1-\beta)$

Principle 1: A polynomial convergence order is acceptable if high accuracy can be practically attainable.

Principle 2: Errors with magnitudes near machine precision are tolerable.

Remark 1: The windowing function need not be in C^∞.

Remark 2: The windowing function need not even be continuous.

Remark 1 can be easily proved if we accept Principle 1, which has already allowed the development of a variety of PDE solvers presented in Ref [3, 4, 9, 10, 23] which have spectral like behavior within the computational domain and acceptable polynomial convergence order at the domain boundaries.

Principle 2 implies Remark 2 which allows a great deal of freedom on the construction of discontinuous windowing functions. Figure 4.3 shows virtually indistinguishable discrete Fourier coefficients (computed in very high precision) of the following functions

$$f_1'(x) = \exp(\sin(4\pi x)) \qquad f_2'(x) = f_1'(x) + \begin{cases} 0 & \text{if} \quad x \leq 1/2 \\ 10^{-15} & \text{if} \quad x > 1/2 \end{cases}$$

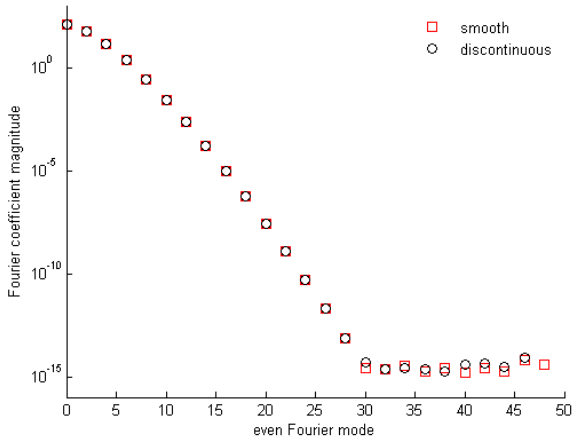

Figure 4.3: Discrete Fourier coefficient magnitudes of a smooth function $f_1^{'}(x)$ and a (mildly) discontinuous function $f_2^{'}(x)$

Even though the discontinuous function $f_2^{'}(x)$ decays slower than $f_1^{'}(x)$, both functions behaves similarly in finite double precision round-off error.

4.2.1 The Optimization Problem

These two remarks provide a heuristic way of choosing a windowing function ϕ , which need not be smooth or even continuous. Particulary, the associated smooth step function ψ (see Figure 4.2) should be sufficiently bandlimited so that its transition region can be well-resolved with $M = 25$ points. This can be restated as the following optimization problem.

For a given W, minimize

$$J(a) = \int_0^{\alpha} \psi^2(x)\,\mathrm{d}x + \int_{1-\beta}^{1} \left(\psi(x) - 1\right)^2\,\mathrm{d}x \tag{4.4}$$

where

$$\psi(x) = \begin{cases} \sum_{k=0}^{W} a_k\,\cos(k\pi x) & \text{if } \alpha \neq \beta \\ a_0 + \sum_{\substack{k=1 \\ k\ odd}}^{W} a_k\,\cos(k\pi x) & \text{if } \alpha = \beta \end{cases}$$

The form of Equation (4.4) allows a semi-analytic solution to the optimal problem : the

stationarity conditions takes the form of the linear system,

$$A\mathbf{a} = \mathbf{b} \tag{4.5}$$

After straightforward algebraic and trignometric manipulations (see Appendix A for a complete computation), the coefficients of a_k can be calculated numerically with high precision.

The entries of $\mathbf{b}$ are given by,

$$b_l = \begin{cases} 2\beta & \text{if } l = 0 \\ (-1)^l \dfrac{2\sin(l\pi\beta)}{l\pi} & \text{if } l \neq 0 \end{cases}$$

and the coefficients of a_l in the equation associated with differentiating with respect to a_k can be represented in coefficient matrix A of $(W+3)/2 \times (W+3)/2$ with the diagonal entries,

$$A_{kk} = \begin{cases} 2(\alpha+\beta) & \text{if } l = k = 0 \\ \alpha + \beta + \dfrac{\sin(2\pi k\alpha)}{2\pi k} + \dfrac{\sin(2\pi k\beta)}{2\pi k} & \text{if } l = k \neq 0 \end{cases}$$

and the off-dioagonal entries by,

$$A_{lk} = \frac{\sin(k+l)\pi\alpha}{(k+l)\pi} + \frac{\sin(k-l)\pi\alpha}{(k-l)\pi} + (-1)^{k+l}\frac{\sin(k+l)\pi\beta}{(k+l)\pi} + (-1)^{k-l}\frac{\sin(k-l)\pi\beta}{(k-l)\pi}$$

Since the coefficient matrix A is poorly-conditioned, numerical implementation of Equation (4.5) involves the *variable-precision arithmetric* (vpa) capabilities of Matlab's Symbolic Math Toolbox, to determine a_ks. The vector $\mathbf{b}$ and coefficient matrix A are initialized as **vpa** and the linear system (4.5) is solved and $\mathbf{a}$ is stored in 'double' data type.

By comparing the windowing function parameters α, β, W and maximum difference of a_ks between FC-Gram implicit window and step-up function ψ (see Table 6.1), the following

optimal parameter can be found.

$$\alpha = \beta = 10/68 \qquad\qquad W = 33$$

produces a smooth step $\psi(x)$ with the desirable properties that

$$\max_{[0,\alpha]} |\psi(x)| < 10^{-15} \qquad\qquad \max_{[1-\beta,1]} |1 - \psi(x)| < 10^{-15}$$

and that $M = 25$ extension points are sufficient to achieve accuracy of FC-Gram. The coefficients $\{a_k\}$ s and $M = 25$ discrete samples of ψ this choice of parameters are presented in Appendix B

Chapter 5

Periodization

The periodization step is the last step in the smooth extension of Section 2.1.1. The simplest periodization which can be performed on windowed extension function is to treat $\widetilde{f}_w$ in Equation (4.2) as samples of a periodic function -i.e. nonoverlapping extension periodization.

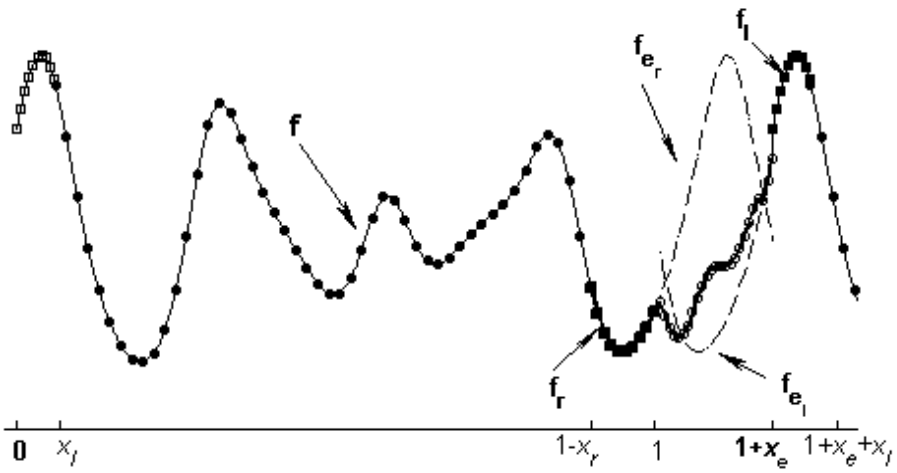

Figure 5.1: Overlapping extension example for the Periodization defined on Equation 5.1

Another choice of periodization with smallest period as shown in Figure 5.1 which can be written in matrix form of

$$\widetilde{f}_{\text{per}} = \begin{pmatrix} I & 0 & 0 \\ 0 & I & 0 \\ 0 & 0 & I \\ \overline{E}_l Q_l^T & 0 & \overline{E}_r Q_r^T \end{pmatrix} \times \begin{pmatrix} f_l \\ f_c \\ f_r \end{pmatrix} \tag{5.1}$$

Chapter 6

Numerical Experiments and Results

This section presents a variety of numerical experiments and results supporting the aim.

1. As discussed earlier in Chapter 3 and 4, resolution of poorly-conditioned numerical computations were achieved via Matlab's **vpa** (variable-precision-arithmetic) with 200 digits of precision. These computation are only needed in the offline phase and the online phase uses only standard double-precision arithmetic.

2. The standard recurrence relation of orthonormal polynomials

$$q_{n+1}(x) = a_{n+1}\left(\left(x + b_{n+1}\right) q_n(x) + c_{n+1} q_{n-1}(x)\right) \qquad n = 2, 3, \ldots$$

   was used to find the appropriate columns of Q and E of Equations (3.2) and (3.3).

3. Once the vector $\mathbf{a}$ of Equation (4.5) and sample values of the bandlimited step ψ were found using vpa, $\widetilde{E}$ of Equation (4.3) was produced and all pre-computed $\widetilde{E}, Q, \mathbf{a}, \psi$ are stored in double-precision for future use.

4. In the online phase, extensions are performed via Equation (5.1) using the database generated in the offline phase.

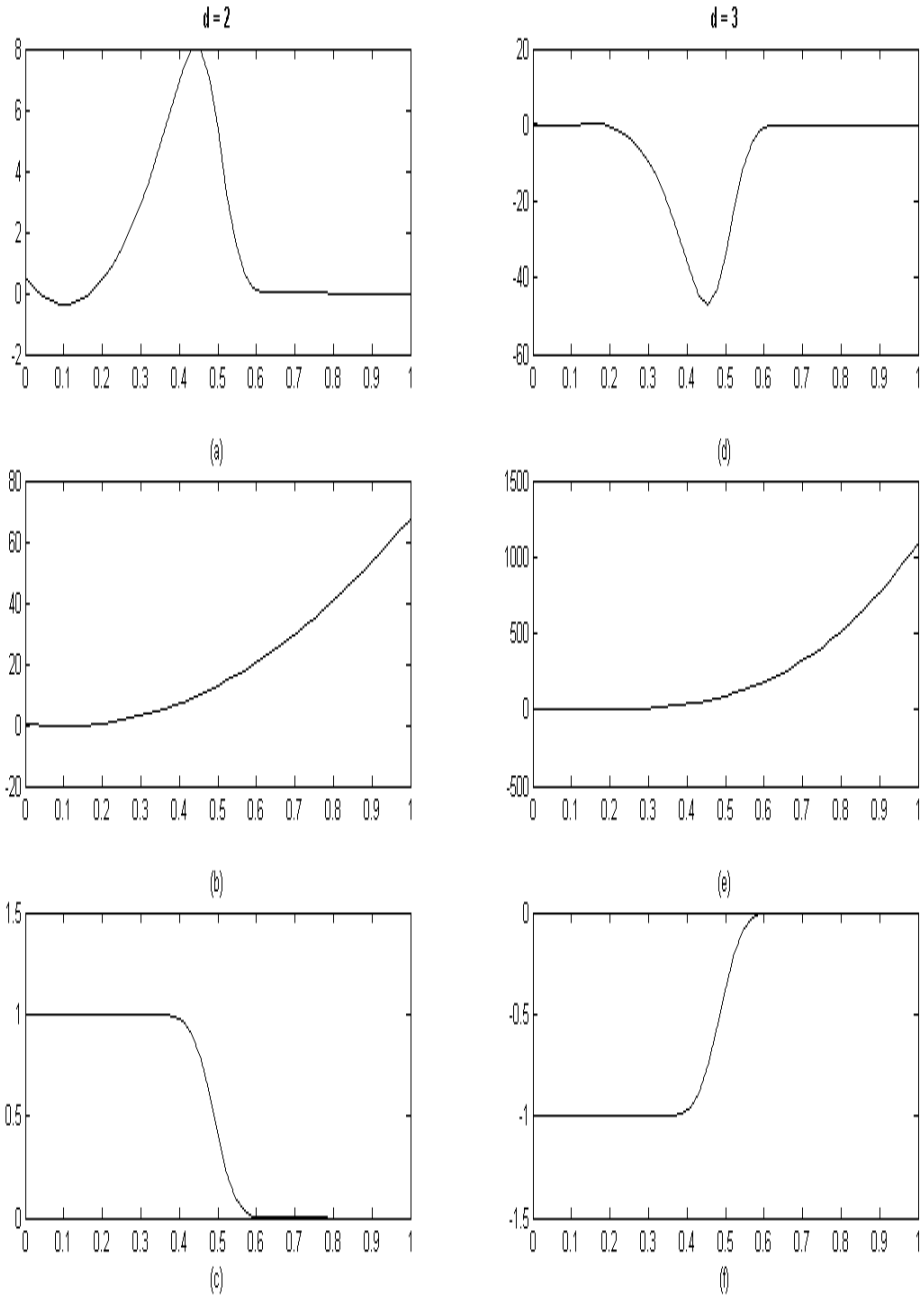

Figure 6.1: In(a), the extended function using FC-Gram method for a polynomial with degree=2. The original function and associated 'implicit' window function are respectively in (b) & (c). Similarly, (d) (e) and (f) are for degree 3.

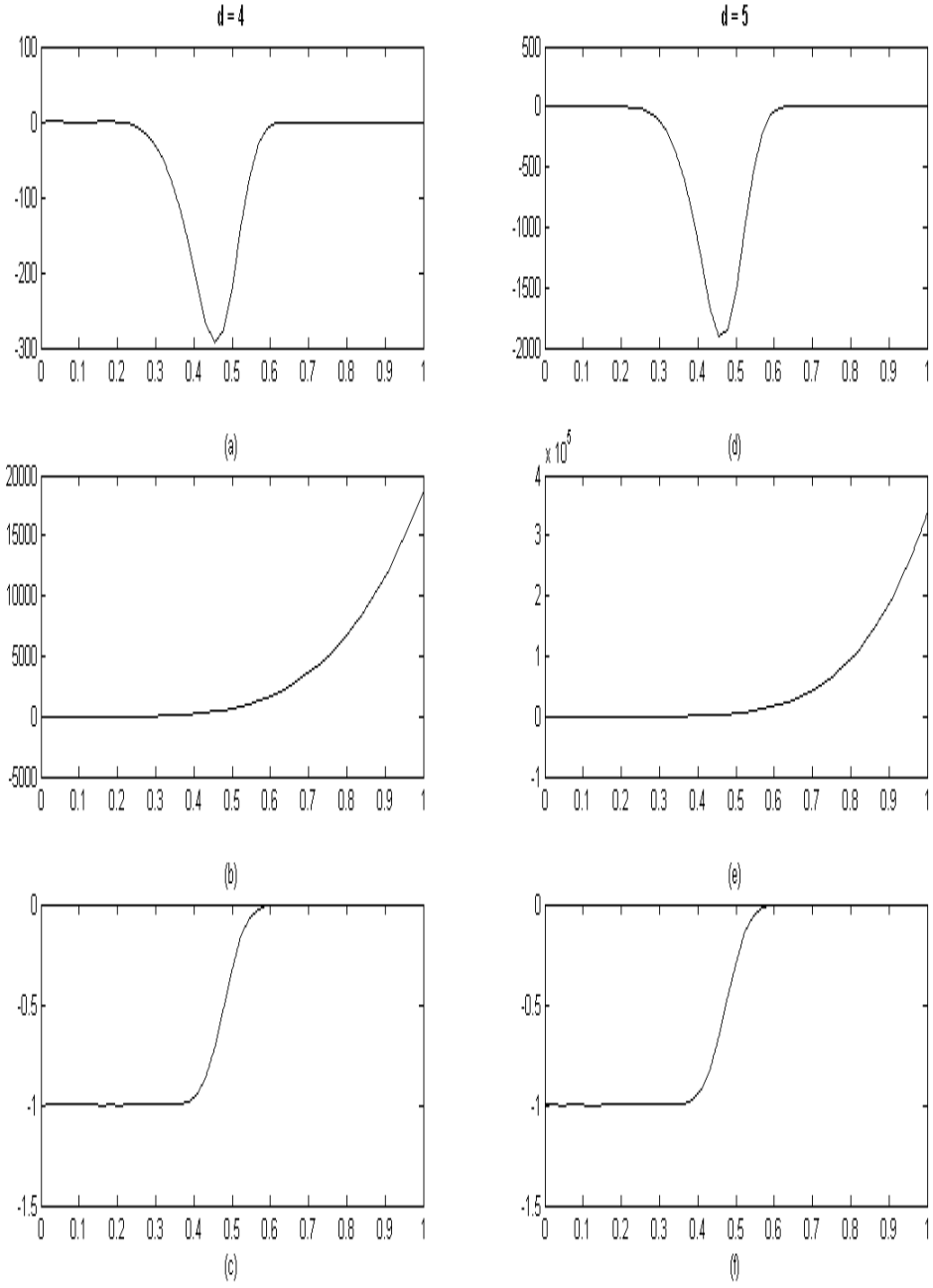

Figure 6.2: In(a), the extended function using FC-Gram method for a polynomial with degree=4. The original function and associated 'implicit' window function are respectively in (b) & (c). Similarly, (d) (e) and (f) are for degree 5.

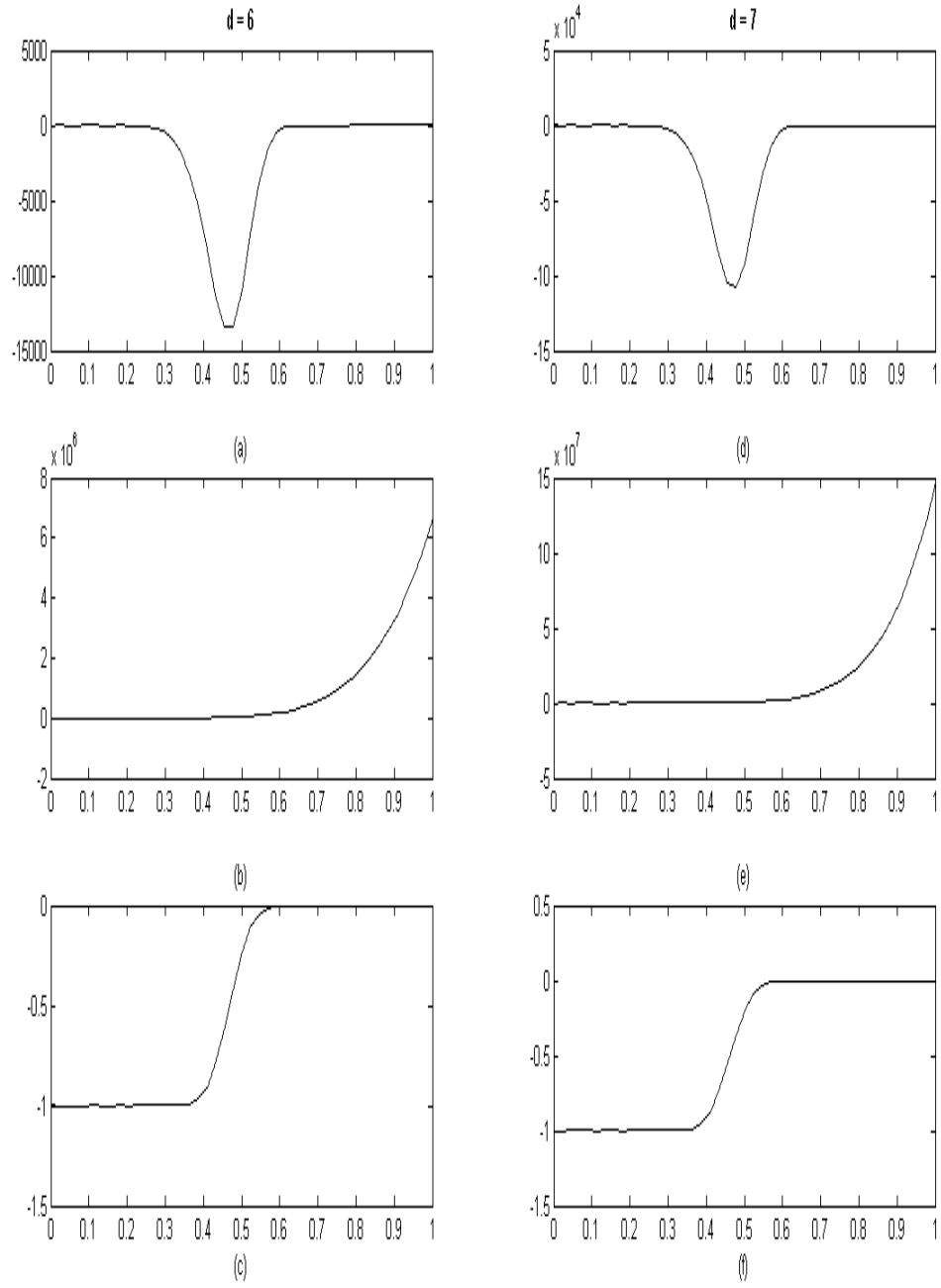

Figure 6.3: In(a), the extended function using FC-Gram method for a polynomial with degree=6. The original function and associated 'implicit' window function are respectively in (b) & (c). Similarly, (d) (e) and (f) are for degree 7.

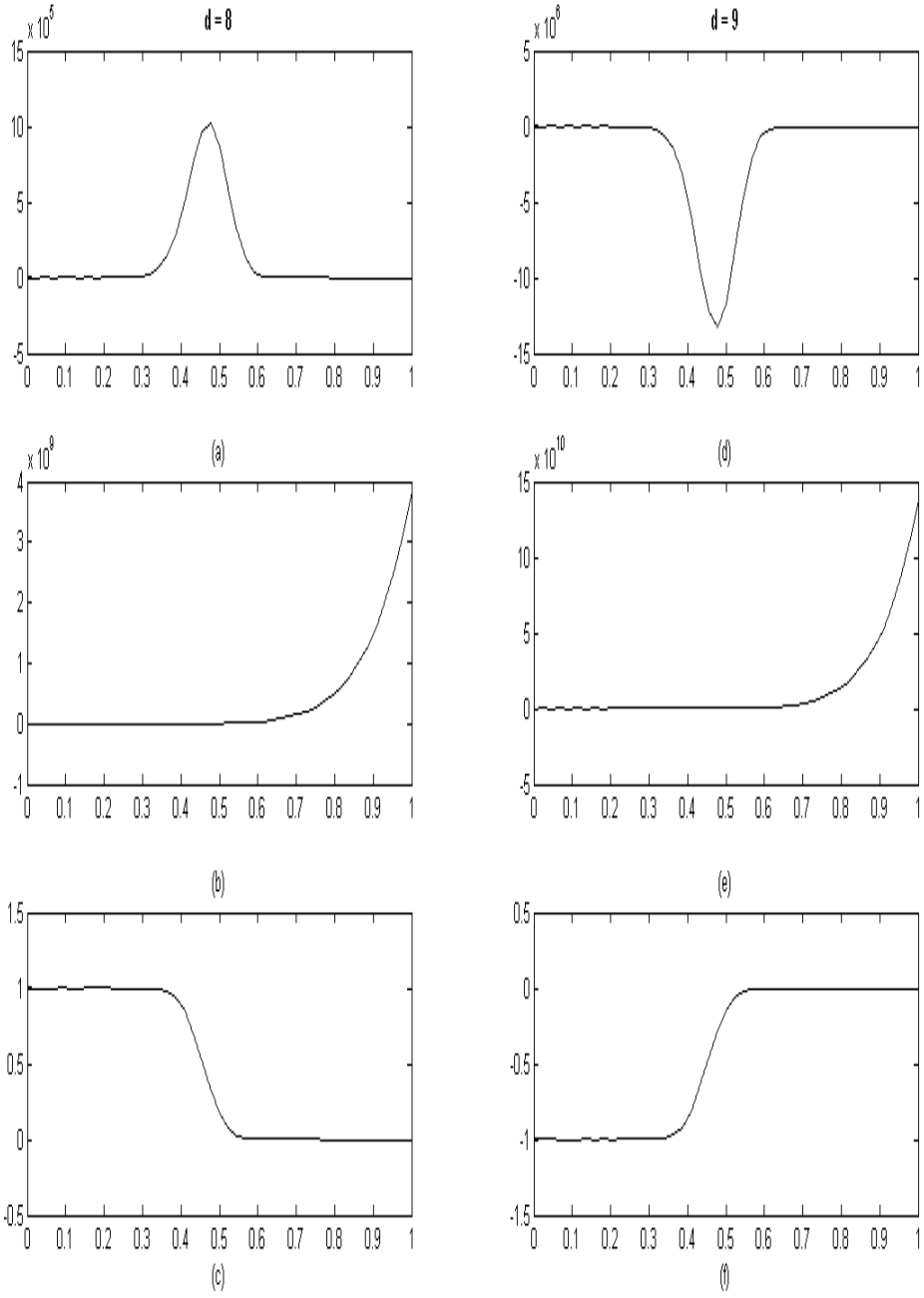

Figure 6.4: In(a), the extended function using FC-Gram method for a polynomial with degree=8. The original function and associated 'implicit' window function are respectively in (b) & (c). Similarly, (d) (e) and (f) are for degree 9.

In order to produce a smooth periodic extension, the windowing function needs to be found. First, as described in Chapter 4 the relationship between the extended function using FC-Gram continuation and associated window function for polynomial functions of degrees 2 to 9 are presented in Figures 6.1 to 6.4.

Because the aim is to present simplified method which act almost as the FC-Gram at the extension, optimal window parameters (α, β, W) were determined by taking the maximum of difference between the samples of ψ at the extension region and associated FC-Gram samples(max-error) with respect to the conditioning of the matrix $\mathbf{A}$ defined in Section 4.2.1. The set of 'best-fit'window parameters of the band-limited step are presented in Table 6.1.

α	β	W	max-error	Conditioning Number of $\mathbf{A}$
0.1	0.1	25	1.14×10^{-2}	1.8982×10^{36}
0.115	0.12	29	1.78×10^{-2}	1.0995×10^{38}
0.12	0.12	29	3.10×10^{-4}	9.5711×10^{37}
0.15	0.15	29	1.86×10^{-2}	1.9408×10^{32}
0.12	0.125	29	1.90×10^{-2}	1.0059×10^{37}
10/68	10/68	33	7.31×10^{-4}	5.4807×10^{37}
0.15	0.15	33	4.1×10^{-3}	1.4434×10^{37}

Table 6.1: The set of 'best-fit' window paramenters of the band-limited step function ψ

The pictorial explanation of such comparison can be seen in Figure 6.5 for $\alpha = \beta = 10/68, W = 33$ of ψ

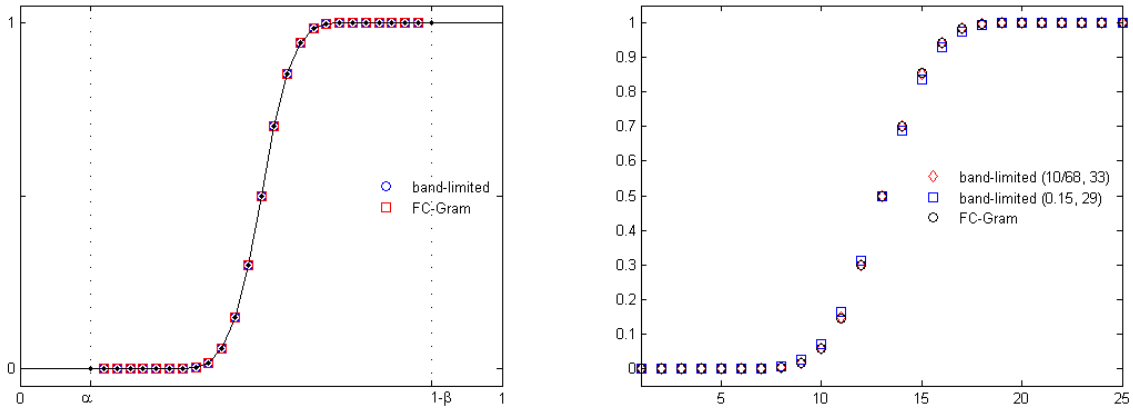

Figure 6.5: Comparison of window functions . In (a), the points labeled 'FC-Gram' indicate the implicit step function obtained when applying the original FC-Gram with $M = 25$ points. The points labeled 'band-limited' indicate the smooth step-up function ψ described in Section 4.2.1 with $M = 25$ extension points and $\alpha = \beta = 10/68, W = 33$. In (b), similar comparison is reproduced with additional band-limited step for $\alpha = \beta = 0.15, W = 29$

With the optimal parameters of ψ, the extension functions were generated for three examples:

$$f_1(x) = x^2$$

$$f_2(x) = \frac{1}{1 + 25(2x-1)^2}$$

$$f_3(x) = \cos(3\pi x)\ \exp\left(\sin(4\pi x)^2\right)$$

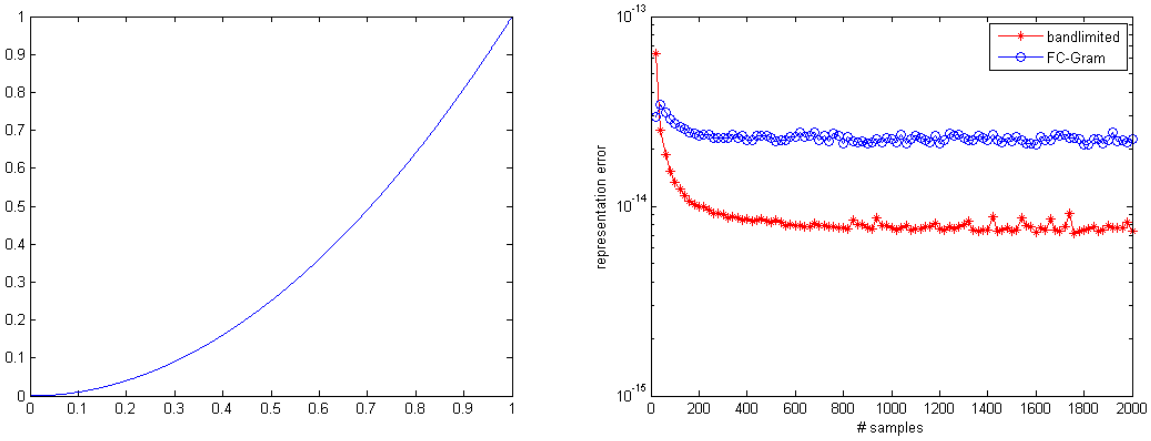

Figure 6.6: In (a), the representation error observed when applying discrete periodic extensions to the function $f_1(x)$ (b). The points labeled 'FC-Gram' indicate the results of applying the original FC-Gram algorithm with $M = 25$ points. The points labeled 'bandlimited' indicate the results of applying the new periodic extension developed in this work using bandlimited step function developed in Section 4.2.1 with $M = 25$ extension points .

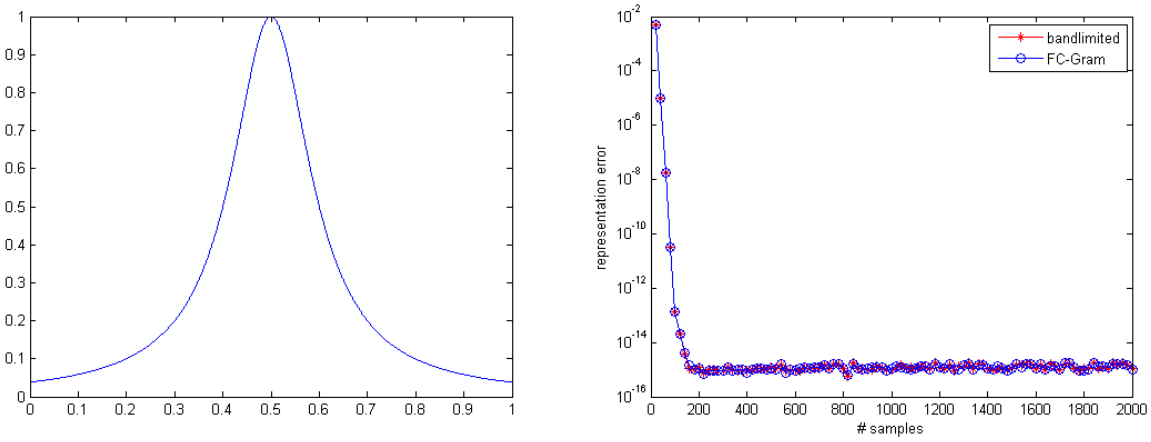

Figure 6.7: In (a), the representation error observed when applying discrete periodic extensions to the function $f_2(x)$ (b). The points labeled 'FC-Gram' indicate the results of applying the original FC-Gram algorithm with $M = 25$ points. The points labeled 'bandlimited' indicate the results of applying the new periodic extension developed in this work using bandlimited step function developed in Section 4.2.1 with $M = 25$ extension points .

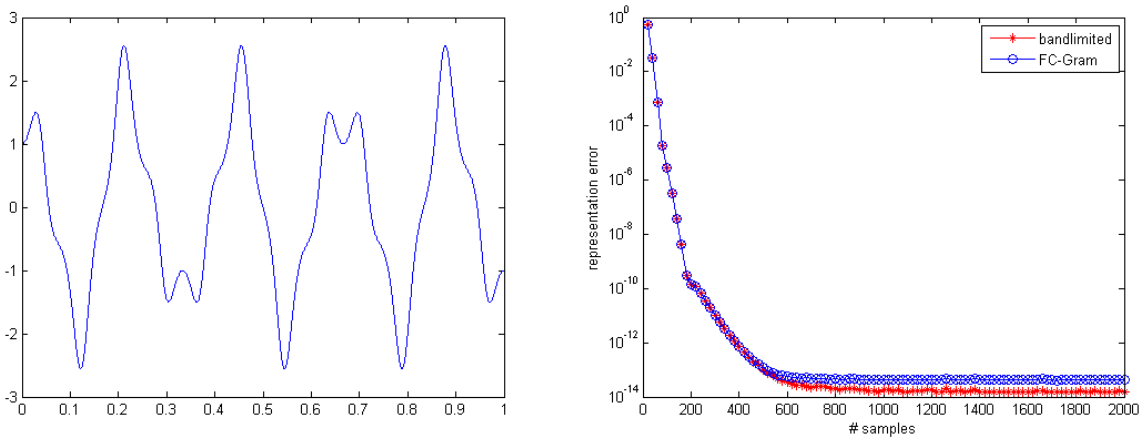

Figure 6.8: In (a), the representation error observed when applying discrete periodic extensions to the function $f_3(x)$ (b). The points labeled 'FC-Gram' indicate the results of applying the original FC-Gram algorithm with $M = 25$ points. The points labeled 'band-limited' indicate the results of applying the new periodic extension developed in this work using bandlimited step function developed in Section 4.2.1 with $M = 25$ extension points .

In each example, the original interval was chosen as $[0, 1]$, and the representation error was compared on a refined grid for the FC-Gram method and the new method band-limited step. In both cases, left-most and right-most grid points N_l and N_r were taken as 10 to produce extension with $M = 25$ points.

Once the extension is known, it is evaluated on a refined grid for various N (10 to 2000) using Fourier interpolation. Figures 6.6 to 6.8 shows the results of representation error for those three examples. Here, notice the representation error was estimated by computing maximum error of the interpolants in the original interval. These plots demonstrate the remarkable similarity of both extension methods. (see Figure 6.9 for extension comparison in $[0, 1.025]$).

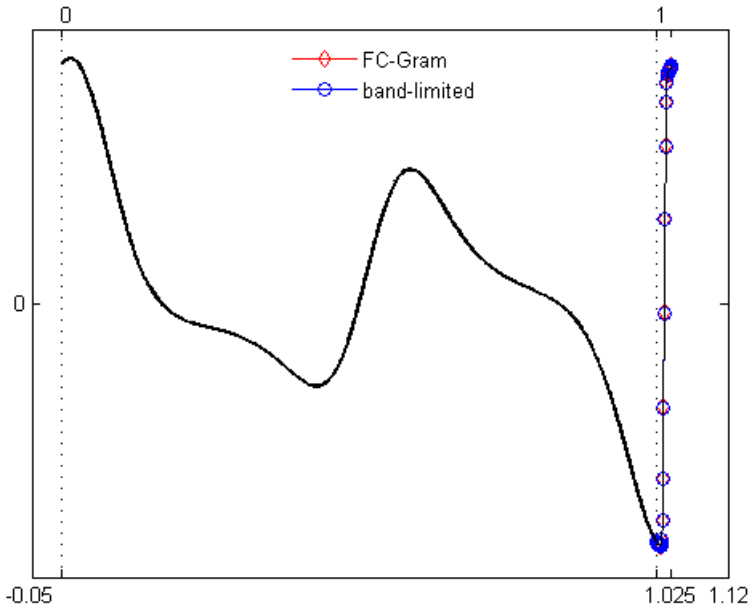

Figure 6.9: Comparison of smooth extension of a function defined on [0,1], using FC-Gram method and new periodic extension developed in this work

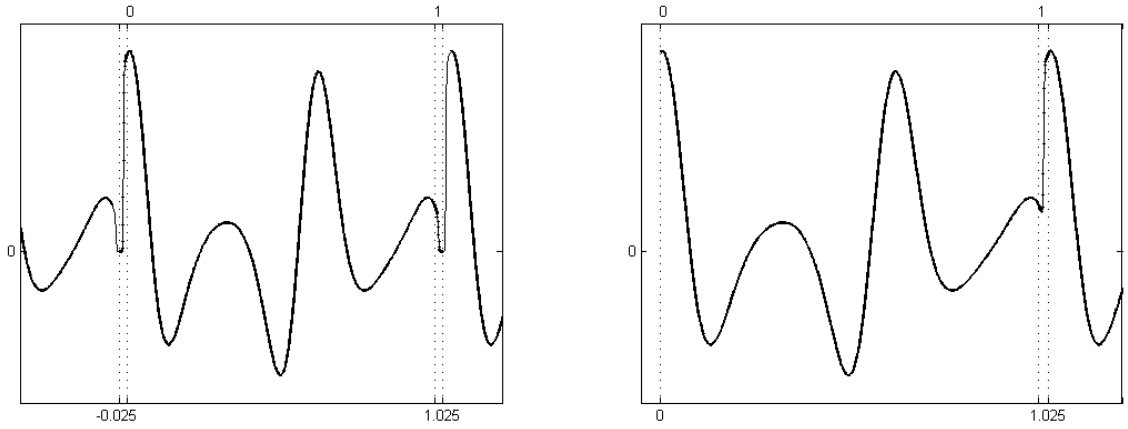

Figure 6.10: In (a), non-overlapping discrete periodic extension of function $f_4(x)$ for the periodization as in Equation (3.4) and in (b) overlapping extension for a small period as defined in Equation (5.1)

Finally, discrete periodic extension with periodization as in Equations (5.1) and (3.4) are presented in Figure 6.10 for $f_4(x) = \cos(2.1\pi x)\ \exp(\sin(1.2\pi x - 5))$.

As stated in the beginning of this Chapter, precomputation phase of bandlimited step requires only $2.5s$ where the 10^{th} order FC-Gram method requires approximately $200s$ [3].

Chapter 7

Conclusion

This work presents a new algorithm for discrete periodic extension of non-periodic signals for use in Fourier-based PDE solvers. The new algorithm, based on a three-step process of smooth extension, windowing and periodization provides a simplified replacement for the existing FC-Gram methodology. In all numerical examples presented in Chapter 6, the new algorithm performed nearly identical to FC-Gram, but with setup time decreased by 98.75%. Although, there is an open question seeking the 'best' method among the new method we presented here and FC-Gram, we conclude this new algorithm provides feasiblility on PDEs solvers construction. We believe this faster and simpler new extension method presented here will have a significant impact on future development of PDE solvers.

Bibliography

[1] Adcock, B., and Huybrechs, D. On the resolution power of Fourier extensions for oscillatory functions. *arXiv preprint arXiv* (2012), 1105–3426.

[2] Adcock, B., Huybrechs, D., and Martin-Vaquero, J. On the numerical stability of Fourier extensions. *arXiv preprint arXiv* (2013).

[3] Albin, N., and Bruno, O. P. A spectral FC solver for the compressible Navier-Stokes equations in general domains I: Explicit time-stepping. *J. Comput. Phys. 230*, 16 (2011), 6248–6270.

[4] Albin, N., Bruno, O. P., Cheung, T., and Cleveland, R. O. Fourier continuation methods for high-fidelity simulation of nonlinear acoustic beams. *J. Acous. Soc. Am. 132*, 4 (2012), 2371–2387.

[5] Boyd, J. A comparison of numerical algorithms for Fourier extension of the first, secomd and thrid kinds. *J. Comput. Phys. 178* (2002), 118–160.

[6] Boyd, J. P. Asymptotic Fourier coefficients for a $\mathcal{C}^\infty$ bell (smoothed-top-hat) & the Fourier extension problem. *J. Sci. Comput. 29*, 1 (2005), 1–24.

[7] Bruno, O., Han, Y., and Pohlman, M. Accurate, high-order representation of comples three-dimensional surfaces via Fourier-continuation analysis. *J. Comput. Phys. 227* (2007), 1094–1125.

[8] Bruno, O., and Prieto, A. Spatially dispersionless, unconditionally stable FC-AD solvers for variable-coefficient PDEs. *J. Sci. Comput.* (2013). In press.

[9] Bruno, O. P. *Fast, high-order, high-frequency integral methods for computational acoustics and elecromagnetics*. Springer, 2003. In topics in computational wave propagation, vol. 31 of lecture notes.

[10] Bruno, O. P., and Lyon, M. High-order unconditionally stable FC-AD solvers for general smooth domains I. Basic elements. *J. Comput. Phys. 229* (2010), 2009–2033.

[11] Canuto, C., Hussaini, M. Y., Quarteroni, A., and Zang, T. A. Spectral Methods : Fundamentals in Single Domains. *Scientifc Computation* (2006).

[12] Chen, Z. *Finite Element Methods and Their Applications*. Scientific Computation. Springer, Berlin, 2005.

[13] Eckhoff, K. S. On a high order numerical method for solving partial differential equations in complex geometrices. *J. Sci. Comput. 2*, 12 (1997), 119–138.

[14] Geer, J., and Banerjee, N. Exponentially accurate approximations using Fourier series partial sums. *J. Sci. Comput. 12: 253–287* (1997).

[15] Gottlieb, D., Shu, C. W., Solomonoff, A., and Vandeven, H. On gibbs phenomenon i : Recovering exponential accuracy from the fourier partial sum of a nonperiodic analytic function. *J. Comput. Appl. Math. 43: 81–98* (1992).

[16] Huybrechs, D. On the Fourier extension of non-periodic functions. *SIAM J. Numer. Anal. 47*, 6 (2010), 4326–4355.

[17] Israeli, M., Vozovoi, L., and Averbuch, A. Spectral multidomain technique with local Fourier basis. *J. Sci. Comput. 2*, 8 (1993), 135–149.

[18] Lele, S. Compact finite difference schemes with spectral-like resolution. *J. Comput. Phys. 103*, 1 (1992), 16–42.

[19] LeVeque, R. J. *Finite Difference Methods for Ordinary and Partial Differential Equations : Steady-State and Time-Dependent Problems*. SIAM, 2007.

[20] Lyon, M. *High-order unconditionally-stable FC-AD PDE solvers for general domains.* PhD thesis, California Institute of Technology, 2009.

[21] Lyon, M. A fast algorithm for Fourier continuation. *SIAM J. Sci. Comput. 33*, 6 (2011), 3241–3260.

[22] Lyon, M. Approximation error in regularized SVD-based Fourier continuations. *Appl. Numer. Math.* (2012).

[23] Lyon, M., and Bruno, O. P. High-order unconditionally stable FC-AD solvers for general smooth domains II. Elliptic, parabolic and hyperbolic PDEs; thoretical considerations. *J. Comput. Phys. 229* (2010), 3358–3381.

[24] Majda, A., Donough, J. M., and Osher, S. The Fourier method for nonsmooth initial data. *Math. Comput. 144*, 32 (Oct. 1978), 1041–1081.

[25] Mattsson, K., Svärd, M., and Shoeybi, M. Stable and accurate schemes for the compressible Navier-Stokes equations. *J. Comput. Phys. 227*, 4, 2293–2316.

[26] Olsson, P. Summation by parts, projections and stability i. *Math. Comp. 64:10351065* (1995).

[27] Olsson, P. Summation by parts, projections and stability ii. *Math. Comp. 64:10351065* (1995).

[28] Oppenheim, A. V. *Signals and Systems.* Prentice-Hall signal processing series, 1983.

[29] Strand, B. Summation by parts for finite difference approximations for d/dx. *J. Comput. Phys. 110:4767* (1994).

[30] Strickwerda, J. C. *Finite Difference Schemes and Partial Differential Equations.* SIAM, Philadelphia, 2004.

[31] Svärd, M., Carpenter, M. H., and Nordström, J. A stable high-order finite difference scheme for the compressible Navier-Stokes equations, far-field boundary conditions. *J. Comput. Phys. 225* (Jul 2007), 1020–1038.

[32] Wagner, T. M. *A very short introduction to the Finite Element Method.* May 4, 2004. Technical University of Munich, St.Petersburg.

Appendix A

Optimization problem of the bandlimited step function

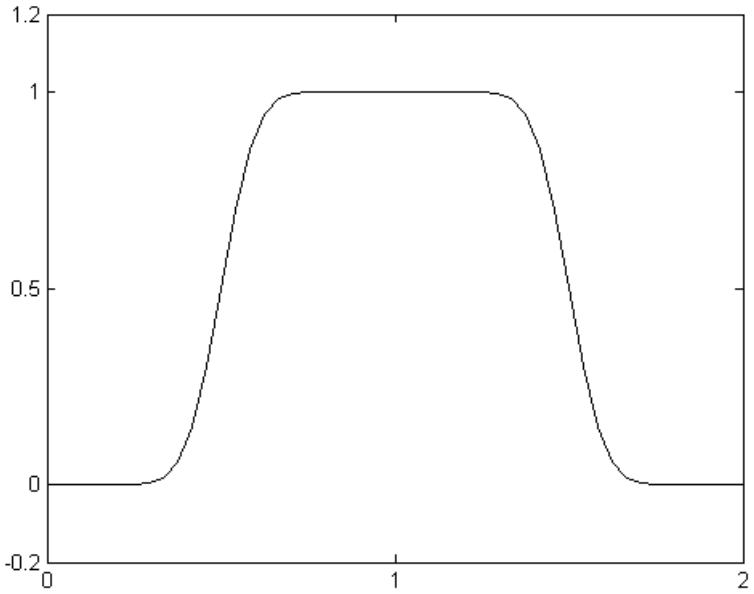

Figure A.1: The windowing function ϕ as defined on Equation (4.1)

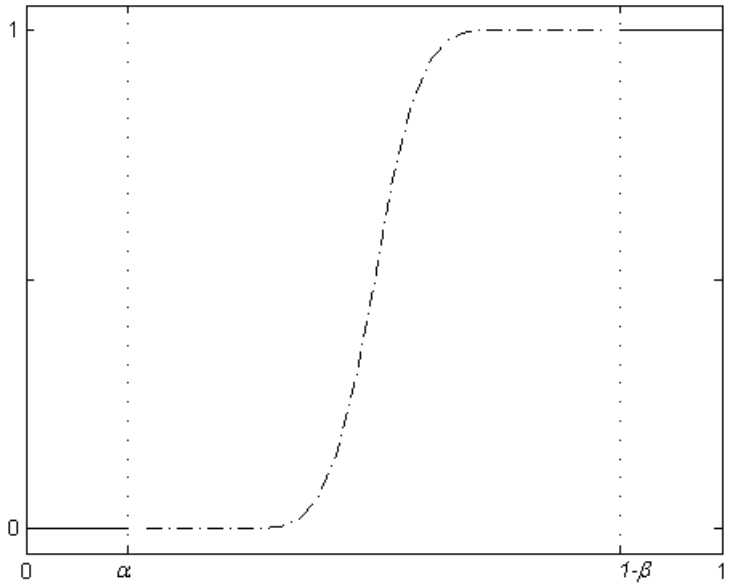

Figure A.2: The bandlimited step-up function ψ on [0,1] (dotted line shows the transition region)

As discussed in Section 4.2.1, because of symmetry (Figure A.1) it is sufficient to analyze the behavior of the step-up function $\psi(x)$.

The step-up function $\psi(x)$ can be formulated as follows:

$$\psi(x) = \sum_{k=-W}^{W} a_k \exp(ik2\pi x/2) = \sum_{k=-W}^{W} a_k \exp(ik\pi x) \tag{A.1}$$

Similarly the step-down function is,

$$\begin{aligned} \psi(2-x) &= \sum_{k=-W}^{W} a_k \exp(ik\pi(2-x)) = \sum_{k=-W}^{W} a_k \exp(i2\pi k)\exp(-2\pi kx) \\ &= \sum_{k=-W}^{W} a_k \exp(-i\pi kx) \end{aligned} \tag{A.2}$$

From the Equations (A.1) and (A.2) we have,

$$a_k = a_{-k} \tag{A.3}$$

In order to determine a_k, let us consider $\overline{\psi}$

$$\overline{\psi(x)} = \sum_{k=-W}^{W} \overline{a_k} e^{-ik\pi x} = \sum_{k=-W}^{W} \overline{a_{-k}} e^{ik\pi x} \tag{A.4}$$

From the Equations (A.3) and (A.4)

$$a_k = \overline{a_{-k}} \tag{A.5}$$

which implies a_k is real

Now, rewrite ψ as,

$$\begin{aligned} \psi(x) &= a_0 + \sum_{k=1}^{W} \{a_k e^{ik\pi x} + a_{-k} e^{-ik\pi x}\} \\ &= a_0 + \sum_{k=1}^{W} a_k 2\cos k\pi x \\ &= \sum_{k=0}^{W} \widetilde{a_k} \cos k\pi x \end{aligned} \tag{A.6}$$

where, $\widetilde{a_k} = 2a_k$ and $\cos k\pi(2-x) = \cos(2k\pi - k\pi x) = \cos(k\pi x)$

In order to determine the behavior of ψ in the transition region (see Figure A.2), $\psi(x)$ needed to be optimized in L^2 norm

i.e. for a given W,

minimize

$$J(a) = \int_0^{\alpha} \psi^2(x)\,\mathrm{d}x + \int_{1-\beta}^{1} (\psi(x)-1)^2\,\mathrm{d}x \tag{A.7}$$

over

$$\psi(x) = \sum_{k=0}^{W} \widetilde{a_k} \cos k\pi x$$

Stationarity requires

$$\frac{\partial J(a)}{\partial a_l} = \frac{\partial J_1(a)}{\partial a_l} + \frac{\partial J_2(a)}{\partial a_l} = 0 \qquad \text{for } l = 0, \ldots, W$$

where

$$\begin{aligned}
\frac{\partial J_1}{\partial a_l} &= \int_0^{\infty} 2\psi(x)\psi'(x)\,\mathrm{d}x \\
&= \int_0^{\infty} 2\sum_{k=0}^{W} \widetilde{a_k} \cos k\pi x \cos l\pi x\,\mathrm{d}x \\
&= \sum_{k=0}^{W} \widetilde{a_k} \left[\frac{\sin(k+l)\pi x}{(k+l)\pi} + \frac{\sin(k-l)\pi x}{(k-l)\pi} \right]
\end{aligned} \tag{A.8}$$

and,

$$\begin{aligned}
\frac{\partial J_2}{\partial a_l} &= \int_{1-\beta}^{1} 2(\psi(x)-1)\psi'(x)\,\mathrm{d}x \\
&= \int_{1+\beta}^{1} 2\sum_{k=0}^{W} \widetilde{a_k} \cos k\pi x \cos l\pi x\,\mathrm{d}x - \int_{1-\beta}^{1} 2\cos(l\pi x)\,\mathrm{d}x \\
&= \sum_{k=0}^{W} \widetilde{a_k} \left[(-1)^{k+l} \frac{\sin(k+l)\pi\beta}{(k+l)\pi} + (-1)^{k-l} \frac{\sin(k-l)\pi\beta}{(k-l)\pi} \right] - 2(-1)^l \frac{\sin(l\pi\beta)}{l\pi}
\end{aligned} \tag{A.9}$$

Now the optimization problem (A.7) can be restated as linear system,

$$A\mathbf{a} = \mathbf{b} \tag{A.10}$$

The entries of $\mathbf{b}$ are given by,

$$b_l = \begin{cases} 2\beta & \text{if } l = 0 \\ (-1)^l \dfrac{2\sin(l\pi\beta)}{l\pi} & \text{if } l \neq 0 \end{cases}$$

The diagonal entries of A are given by,

$$A_{kk} = \begin{cases} 2(\alpha+\beta) & \text{if } l = k = 0 \\ \alpha + \beta + \dfrac{\sin(2\pi k\alpha)}{2\pi k} + \dfrac{\sin(2\pi k\beta)}{2\pi k} & \text{if } l = k \neq 0 \end{cases}$$

and the off-dioagonal entries by,

$$A_{lk} = \frac{\sin(k+l)\pi\alpha}{(k+l)\pi} + \frac{\sin(k-l)\pi\alpha}{(k-l)\pi} + (-1)^{k+l}\frac{\sin(k+l)\pi\beta}{(k+l)\pi} + (-1)^{k-l}\frac{\sin(k-l)\pi\beta}{(k-l)\pi} \tag{A.11}$$

Appendix B

Coefficients of the bandlimited step function

The bandlimited step function ψ used in this work definde through the minimization procedure of section 4.2.1 with parameters $\alpha = \beta = 10/68$ and $W = 33$. The coefficient vector $\mathbf{a}$ produces step function ψ with maximum error less than 10^{-15} on $[0, \alpha] \cup [1 - \beta, 1]$ is as

follows:

$$a_0 = +5.000000000000000e-01 \qquad a_1 = -6.283760496513301e-01$$

$$a_3 = +1.886901484585697e-01 \qquad a_5 = -9.180189543320520e-02$$

$$a_7 = +4.778139936895210e-02 \qquad a_9 = -2.427279866349165e-02$$

$$a_{11} = +1.158461009032351e-02 \qquad a_{13} = -5.082243688315459e-03$$

$$a_{15} = +2.016998130403431e-03 \qquad a_{17} = -7.139361515410136e-04$$

$$a_{19} = +2.220952963675281e-04 \qquad a_{21} = -5.970396023600737e-05$$

$$a_{23} = +1.357963576915037e-05 \qquad a_{25} = -2.540632708684190e-06$$

$$a_{27} = +3.754434177688331e-07 \qquad a_{29} = -4.110209417836622e-08$$

$$a_{31} = +2.964884851916418e-09 \qquad a_{33} = -1.057658328494815e-10$$

The values of ψ at the $M = 25$ sample points in $(\alpha, 1-\beta)$ are as follows.

$$\begin{aligned}\psi(\alpha + ih) = \big(&+3.457318908265273e-15,\ +9.704955199681219e-12,\ +2.201350338787916e-09,\\ &+1.417225475469217e-07,\ +3.998374644825824e-06,\ +6.140384598655076e-05,\\ &+5.830414065986963e-04,\ +3.717643891575275e-03,\ +1.686099479058001e-02,\\ &+5.676516735376654e-02,\ +1.467665490567647e-01,\ +3.001925106972634e-01,\\ &+4.999999999999998e-01,\ +6.998074893027363e-01,\ +8.532334509432356e-01,\\ &+9.432348326462333e-01,\ +9.831390052094202e-01,\ +9.962823561084246e-01,\\ &+9.994169585934016e-01,\ +9.999385961540140e-01,\ +9.999960016253554e-01,\\ &+9.999998582774522e-01,\ +9.999999977986493e-01,\\ &+9.999999999902947e-01,\ +9.999999999999968e-01\ \big)^T\end{aligned}$$